A Method to Minimise Spurious Background Signals in Gas Detectors based on Correlation Spectroscopy using a Fabry Perot by Bandpass Filter Shape Optimisation.

E. Vargas-Rodríguez, and H. N. Rutt

Optoelectronics Research Centre,

University of Southampton, Mountbatten Bldg., SO17 1BJ, Southampton, UK

fax: +44 (0) 2380593149, email: evr@orc.soton.ac.uk

Abstract

The parasitic background signal produced by gas detectors using a Fabry-Perot Interferometer (FPI) as a modulator is shown to be very sensitive to the infrared band pass filter characteristics. This parasitic signal is generally the feature limiting the sensitivity of such devices. We review this problem, and provide a general approach to filter choice which minimises the background amplitude for this kind of detection system. It is shown that in general filters with very abrupt transitions from the stop to pass band are in fact undesirable, and fortuitously the optimum choice of filter leads to easily realised, low cost designs.

Keywords: Gas detection, Background Modulation; Amplitude Modulation; Rotational Lines; Fabry Perot Interferometer.

1. Introduction

Several designs of infrared absorption based gas detector use a Fabry-Perot Interferometer (FPI), sometimes called a comb filter, to modulate the incident light. Generally, this technique is applied in the region from 2-8 μm where many gases have their fundamental absorption bands. Some examples of detectors using this kind of modulator are given in [1-4]. In these systems, the modulation is induced by matching the FPI's fringes with very well defined rotational absorption lines of a target molecule (Fig. 1a). Well resolved absorption lines with Lorentzian line shapes are characteristic of most diatomic and linear molecules, i.e. CO_2, CO, N_2O, and some specific absorptions bands of symmetric top and spherical top molecules eg. NH_3, CH_4 at one atmosphere pressure. In order to obtain modulation the FPI fringes should be shifted along the wavenumber axis (Fig. 1b). This shift is obtained by scanning the FPI cavity over one free spectral range (*FSR*). The transmission through the system is given by

$$I_D(d) = \int_0^\infty I_{FP}(v,d)T(v)Fil(v)S(v)dv\,, \tag{1}$$

where v is the frequency expressed in wavenumbers (1/cm), $I_{FP}(v,d)$ describes the FPI fringe pattern, the filter transmission is given by $Fil(v)$, the transmission through the gas pathlength is defined by $T(v)$, and the source spectral profile is defined by $S(v)$. In $I_{FP}(v,d)$ the FPI cavity length, which is scanned over a range from 0 to one *FSR*, is given by *d*. Thus, a transmission value $I_D(d)$ is obtained for each value of *d*, producing a signal similar to the example shown in Figure 2. In this example the transmission was evaluated using the rotational absorption lines and the FPI pattern

shown in Figure 1, and for simplicity $Fil(v)$ and $S(v)$ were considered to be equal to unity. Finally, the amplitude modulation is taken as the difference between the maximum and the minimum values of $I_D(d)$.

In general, systems using a FPI modulator need an infrared band pass filter to isolate the molecular absorption band of interest. This filter will affect the amplitude modulation, especially the case of the background modulation. In this case no gas is present in the system, ideally no amplitude modulation should be produced, and $T(v)=1$. Since the rotational absorption lines are not present, the modulation is induced by the interaction of the FPI fringes, the source and the filter. As the concentration of the target gas increases the amplitude modulation is less affected by the filter characteristics, and is more affected by the interaction of the FPI fringes and the rotational absorption lines. The optimisation of the filter design is focused on obtaining the maximum amplitude modulation with gas present and the minimum background amplitude possible when it is absent. In general, the background optimisation task is carried out by trial and error, and does not guarantee the best possible result. It appears that sensitivity of background amplitude modulation to the filter characteristics has not previously been explored in the literature. In this work we present a simple analytical approach that describes the underlying reasons why for some filters the background amplitude is severe, and gives guidance on the choice of optimised filters. We show that relatively simple low cost filters are often a better choice than very steep sided filters in this application.

2. Description of the Gas detector with FPI modulator

In these detectors, the FPI will produce a pattern of fringes which are symmetrical and equidistant [5]. The FPI's transmission pattern for normal incidence, I_{FP}, is given by the Airy formula [5] expressed by

$$I_{FP} = \frac{1}{1 + \frac{4R}{(1-R)^2}\sin^2\left(\frac{4\pi\ nd}{2\lambda}\right)}, \tag{2}$$

where R is the mirror reflectivity, nd is optical thickness of the FPI, and λ is the wavelength in the air. One other important parameter that needs to be defined here is the separation between the FPI's fringes which is known as the Free Spectral Range (*FSR*), and can be expressed in term of wavenumbers as [5]:

$$FSR = \frac{1}{2nd}. \tag{3}$$

In a very simple approach, if we know the average separation between the rotational absorption lines of a gas in a specific range, we can match it with the *FSR* and therefore, the optical thickness (*nd*) of the FPI can be derived. The optimal value of the parameter *FSR* requires further analysis, since in fact the rotational line spacing is not exactly constant, primarily owing to changes in the molecular rotational constants between the ground and excited states. Therefore, as the rotational absorption lines are not equally spaced it is important to select the optimal *nd* parameter value to assure the maximum amplitude modulation when the FPI cavity length is scanned by $\lambda/2$. However, in this work we will not discuss this factor

further, but rather concentrate on the separate issue of band-pass filter choice. A segment of a simulated CO_2 transmission spectrum and the FPI's fringes are shown in Figure 1. In this figure it is possible to observe how the FPI's fringes are shifted along the wavenumber axis showing the effect of scanning the cavity length from 0 to $\lambda/2$ [6].

As the rotational lines of the molecules are not equally spaced it is necessary to isolate a specific part of the absorption spectrum, ideally a region where the lines present approximately constant separation. In addition, the filter is needed in order to reduce the sensitivity of the detector to absorption due to different molecules ('cross sensitivity'). For example, it is undesirable that a CO detector responds to absorptions due to CO_2 or H_2O. Whilst the correlation mechanism provides significant rejection of response to other molecular species, the band pass filter provides additional rejection and prevents overload of the infrared detector by broad-band, unmodulated radiation carrying no information.

The simplified response of the system was described in the previous section and represented by (1). A more complete form for the transmission response is given by

$$I_D(R, nd, d) = \int_0^\infty I_{FP}(v, R, nd, d) T(v) Fil(v) S(v) dv, \tag{4}$$

where d represents the length of the FPI cavity, scanned from 0 to $\lambda/2$. As stated previously the design goal is to have the maximum amplitude of $I_D(R, nd, d)$ possible

when the gas is present, $T(v) \neq 1$. However, in addition, we need to minimize the amplitude of the background amplitude when $T(v) = 1$.

Intuitively designers tend to choose filters with steep sides and high out of band rejection, seeking to minimise cross sensitivity to other gases. However, simulation by numerical evaluation of (4) showed that such choices frequently produce very severe background signals in the absence of any gas. Hence it was necessary to find an analytical method to decide which filter characteristics will reduce the background amplitude. In the next section we present a mathematical approach that helps to select the filter that will produce the lowest background amplitude modulation. This approach does not affect the amplitude modulation when the gas concentration is increased, so that the detector sensitivity is not reduced.

3. Filter selection, a general approach

The integrated transmission of the system detector defined by equation (4), can be simplified for the particular case of the background modulation and rewritten as

$$I_D(R, nd, d) = \int_0^\infty I_{FP}(v, R, nd, d) Fil(v) S(v) dv, \tag{5}$$

since the rotational absorption lines are not present, as $T(v) = 1$. Furthermore, if we consider fixed values of *nd* and *R*, thus equation (5) can be simplified to

$$I_D(d) = \int_0^\infty I_{FP}(v, d) Fil(v) S(v) dv. \tag{6}$$

As the cavity needs to be scanned to induce modulation, d must be varied, and shift of the FPI's fringes over the wavenumber axis (Δv) is produced (Fig. 1). Therefore for each value of d we will shift the FPI fringes in Δv, hence it is useful to express (6) as

$$I_D(\Delta v) = \int_0^\infty I_{FP}(v, \Delta v) Fil(v) S(v) dv . \tag{7}$$

Now, considering that the width of the FPI's fringes and their symmetry do not vary when they are shifted over one *FSR*, the response of the system is optimised for a FPI cavity length scan of $\lambda/2$, and making $G(v) = Fil(v)S(v)$, equation (7) can be rewritten as

$$I_D(\Delta v) = \int_0^\infty I_{FP}(\Delta v - v) G(v) dv . \tag{8}$$

The background amplitude modulation problem has been reduced to (8) which has the form of a simple convolution. Hence, the identification of the filter shape that produces the lowest background amplitude can be determined by evaluating the Fourier Transform (FT) of equation (8). We recall that the FT of a convolution ($*$) is given by

$$\mathrm{FT}\{I_{FP}(v) * G(v)\} = I_D(\omega) = I_{FP}(\omega) G(\omega). \tag{9}$$

Therefore, it is expected that the background amplitude will be minimum when $I_D(\omega)$ tends to zero. We first consider $I_{FP}(\omega)$, which represents the FT of the FPI's

fringe pattern given by the Airy formula (2), whose FT will produce a series of equidistant spectral lines (these lines must not be confused with the gas 'spectral lines') since the Airy function can be expressed as a cosine series [7]. Hence in order to have $I_D(\omega)$ near to zero, $G(\omega)$ should have a response approximately equal to zero at the frequencies where the impulses due to the FT of equation (2) occur. The FT of the Airy function for nd = 0.28 cm, and R = 0.45 is shown in Figure 3. It can be observed that the impulse due to the fundamental frequency of equation (1) is exactly at 2nd, which is the inverse of the FSR.

4. Examples of the general filter selection approach

In this section some simulated results of the filter selection approach are presented. In the first case, let us to consider a set of three ideal filters, all of them with the same full-width-at-half-maximum bandwidth (Fig. 4). In this example, the parameters of the FPI are, as before, nd = 0.28, and R = 0.45 (Fig. 1); The source is considered to be flat, therefore, $G(\omega) = Fil(\omega)$. This is a good approximation for realistic, common thermal sources over the bandwidth of interest (note that for some infrared LED sources this approximation may be invalid.) The FTs of the three filters are shown in Figure 5a, here it is possible to observe that the sinc function FT of the square filter has the sidelobes with the biggest magnitude. Based on our approach, we expect that the filter that produces the lowest background amplitude is that with the lowest magnitude in the regions near to $m2nd$, where m=1, 2, 3…. In order to clarify this, a detail of the filters' FTs around 2nd is shown in Figure 5b. From this figure we can determine that the filter that will produce the biggest background amplitude response will be the square filter (F1), because it has the biggest magnitude in the

region of interest. Conversely, the filter that will produce the lowest background amplitude will be F3.

In figure 5 we see that the FTs of the filters have many sidelobes and therefore many points where the FT magnitude is close to zero. At first sight a method to minimise the background signal is to position these zeroes so as to coincide with the lines in the Fourier Transform of the Airy function. This will produce a very low background modulation for practically any filter with a bandwidth equal to an exact integral multiple of the *FSR*. The big disadvantage of doing this is that the bandwidth of the filter needs to be specified to an accuracy of <<*FSR*, which is generally impractical. It complicates the filter design and requires extremely precise process control increasing the cost. So, for simplicity, the best filter is considered to be the one with the lowest sidelobe magnitude in the region around (2*nd*). Minimisation of the sidelobe amplitude is a practical option, whilst precise location of the zeroes is not.

In order to demonstrate the efficacy of the general filter approach, the background amplitude modulation for each of the filters was evaluated as a function of the optical thickness *nd*, by numerical integration of (4) and the simulated results are shown in Figure 6. $T(v)$ was generated from an model including all high-order spectroscopic constants, hot bands and significant isotopomers, using *J*-dependent Lorenzian broadening and a temperature of 295K [8,9]. Owing to the highly structured form of the integrand, small frequency intervals must be used and the integration is time consuming. It is clear here that the system with the biggest background amplitude modulation is when the square filter is used. In contrast, the

lowest background amplitude is obtained using the filter F3. Finally, the amplitude modulation of the system as a function of the gas concentration (ppm) is shown in Figure 7, here a gas path length of 3.5 cm at one atmosphere was used. From this figure, we can observe that when the filter with steepest sides is used eg. F1, the amplitude modulation for low concentration levels (background inclusive) is severely affected by the filter characteristics. The second is that as the concentration increases the system is less sensitive to the filter characteristics. It can be seen that the modulation for higher gas concentrations is practically the same for all the filters, which means that selecting a filter which produces a low background amplitude modulation does not reduce the detector response when the target gas is present. So, we can deduce that when a filter with 'soft' sides is used (eg. F3), the amplitude modulation for low concentration levels is governed mainly by the gas concentration rather than by the filter characteristics. This produces a far more linear detector response to the gas concentration since the background amplitude can be reduced over an order of magnitude depending of the filter, and so the gas detector performance is greatly improved. For example, the amplitude modulation using F1 is quite flat from 0 to around 60 ppm (Fig. 6), making it essentially impossible to determine the correct gas concentration. In contrast, the amplitude modulation is described by a straight line when F3 is used. In general, all these results are in very good agreement with the predictions given by our approach.

In a second example of the general filter approach, we consider the important case of a CO detector. In this case, the background amplitude modulation considering the ideal performance of a standard commercial filter set [10] was evaluated. As in the first example, a flat broad band source was used, and the optical thickness was fixed

at *nd*=0.14 cm. As previously stated, the problem is to decide what filter is the best for the application. Using our approach, just the FT of these filters needs to be evaluated and checked in the region close to 2*nd*. The performance of the commercial filter set is shown in Figure 8a, and a detail of the FT of the filters in the region close to 2*nd* is presented in Figure 8b. Hence, it is possible to predict that F3 will have the worst background amplitude, while the other filters will have lower and similar background amplitudes. The computed background amplitudes for these filters are given in Table 1, which are in good agreement with the predictions, since F3 has background amplitude around 15 times larger than that produced by the other filters.

Table 1- Computed Background Amplitude for a CO detector.

Filter	***nd***	***R***	**Background Amplitude**
F1	0.14	0.5	1.14×10^{-4}
F2			1.70×10^{-4}
F3			2.31×10^{-3}
F4			1.50×10^{-4}

Finally, a further benefit of the technique is that the effect of filter manufacturing tolerances is easily investigated. As steep sided filters, which have a more complex design and are frequently most sensitive to manufacturing errors, are not required, simple three or even two cavity filters [11] are a good choice for the application. In order to show how robust the system is to filter manufacturing error, let us to consider an ideal filter that transmits in the 4.3 μm region [10] where the

strong antisymmetric stretch, parallel absorption band of CO_2 lies. The thicknesses of the most sensitive layers of the filter were varied intentionally to compute the performance of filters with simulated manufacturing errors. TFCalc software [12] was used to compute the most sensitive layers of the filter. In Figure 9 the performance of the ideal filter and of two filters with a thicknesses error in a highly sensitive layer, are shown. To determine if the background amplitude modulation will be seriously affected by errors in the filter, the FT approach is applied. Here, let us to consider the same optical thickness as in example one, nd=0.28. Hence, we need to consider the magnitude of the filters' FT in the region around 2nd, where the fundamental frequency of the Airy function falls. A detail of the FT around 2nd=0.56 is presented in Fig 10. We see that the magnitudes of the filters' FT are similar, thus similar background amplitude modulation will be obtained with the three filters. A full simulation of the amplitude modulation, for the three filters, as a function of the concentration is shown in Figure 11. It is possible to observe that for a 0 ppm CO_2 concentration, which corresponds to the background case, the system response has a similar value for all the filters, which is in accordance with the prediction given by our approach. Also, from Figure 11 it can be observed that if the filter's transmission is seriously reduced by manufacturing errors in layer thicknesses, only the amplitude modulation response is reduced. This is reasonable since the average transmission through the system is reduced. Consideration of the FT of the filter bandpass shape, including errors, enables us to safely conclude that the only effect of the errors is that due to reduced transmission, and no degradation of the background signal, and hence minimum detectable concentration, will occur other than through reduced signal-to-noise resulting from the reduced transmission. These results considerably relax the

filter design requirements for this kind of detector, and eliminate the need for time consuming evaluation of equation (5) for many different cases.

5. Conclusions

The effect of the filter characteristics on the background amplitude in gas detectors using an FPI as a modulator in a form of correlation based device has been analysed. This background modulation determines the minimum detector sensitivity. From this analysis we present a mathematical procedure to show why some filters produce high background amplitudes, and we present a simple approach to select the best filter for this type of detector. An important point derived from this work is that narrow band, with very steep sided, 'square' shaped pass-bands filters will produce high background modulation, because the FT of these filters has high sidelobes, whilst filters with more gradual transitions to the stop-band have low sidelobes. This reduces the cost of the system, because in general filters with 'soft sides' are the best choice for the application and these filters are relatively cheap and easy to fabricate. The method also provides a quick and easy way to evaluate the effect of manufacturing tolerances on the IR filters, by observing their effect on the Fourier Transform of the bandpass function, without extensive full scale simulations.

6. Acknowledgements

E. Vargas-Rodríguez is grateful to the Mexican National Council for Science and Technology (CONACyT) for a student research grant.

References

1. J. P. Dakin, C. A. Wade, D. Pinechbeck, J. S. Wykes, "A novel fibre methane sensor," *SPIE* Vol **734**, 254-260 (1987).
2. J. P. Dakin 1988, "Review of Fibre Optic Gas Sensors", The Plessey Company PLC, UK (1988).
3. W. Jin, G. Stewart, B. Culshaw, and S. Murray, "Source-noise limitation of fiber-optic methane sensors," *Applied Optics* **34**(13), 2345-2349 (1995).
4. W. Jin, G. Stewart, B. Culshaw, S. Murray, and D. Pinchbeck, "Absorption measurement of methane gas with a broadband source and interferometric signal processing," *Optics Letters* **18**(16), 1364-1366 (1993).
5. M. Born, and E. Wolf, "*Principles of Optics,*" Pergamon Press, Great Britain, pp 323-333 (1965).
6. E. Hecht, "*Optics,*" Addison Wesley Longman, USA, pp 416-418 (1998).
7. J. M. Vaughan, "*The Fabry-Perot Interferometer History, Theory, practice and applications*," Adam Hilger, USA, pp 97-102 (1989).
8. L. S. Rothman, R. L. Hawkins, R. B. Wattson and R. R. Gamache, "Energy Levels, Intensities, and Linewidths of Atmospheric Carbon Dioxide Bands," *Journal of Quantitative and Radiative Transference* **48**(5/6), 537-566 (1992).
9. C. D. Mansfield, "*An Investigation into the Viability of an Infrared Diagnostic Instrument for Measuring the CO_2 Isotope Ratios in Breath*," PhD thesis, University of Southampton (2000)
10. G. J. Hawkins, private communication (2003).
11. H. A. Macleod, "*Thin-Film Optical Filters*," Institute of Physics Publishing, Bristol, pp 267-306 (2001).

12. TFCalc, Software Spectra, Inc., http://www.sspectra.com/, last accessed 26/10/2004.

Authors Biographies

First Author

Everardo Vargas-Rodriguez took his degree in Electronic Engineering at the Tecnologico de Celaya. Afterwards he completed an MSc in Instrumentation at the University of Gunajuato (1st class honours, year prize), Mexico. In 2002, he moved to United Kingdom where he joined the ORC at the University of Southampton to study for PhD in optoelctronics. His research area involves the design of Pyroelectric Detectors with Integrated FPI MEMS Modulator.

Second Author

Professor Rutt took both his BSc and PhD at Southampton University, in the course of the latter building the first optical parametric oscillator to operate in the UK, and the first successful mid infrared OPO. He then spent three years in a University in Brazil establishing a laser research group. Professor Rutt returned to the UK in 1973 and joined the Atomic Energy Authority at Culham Laboratory, working on novel infrared gas lasers for the sixteen micron region. Many novel lasers were discovered and characterised during this period, and some scaled up into 'user friendly' systems for use elsewhere. Prior to leaving Culham Laboratory he was Division Head of Beam Science and Technology, encompassing both the laser beam and ion beam work (mainly H- and D- sources). Prof Rutt took up the newly established Rank Chair of Infrared science and Technology at Southampton University in January 1992. The group is establishing a broad range of work in novel sources, instruments and systems in the mid and far infrared.

Figure Captions

Figure 1- FPI's fringes and rotational lines due to CO_2. a) Absorption lines are matched to the FPI's fringes. b) FPI's fringes shifted along the wavenumber axis. The CO_2 spectrum is shifted up 0.4 units for clarity.

Figure 2- Simulated transmission through the system as a function of the cavity length d.

Figure 3- Fourier Transform of the Airy Function.

Figure 4- Simulated performance of three ideal filters.

Figure 5- Fourier Transforms of both the ideal filters and the Airy Function. a) Positive frequencies of all the spectra; b) detail of the filter spectrum in the region of the fundamental frequency of the Airy Function.

Figure 6- Background Amplitude Modulation as a function of nd.

Figure 7- Amplitude Modulation as a function of the gas concentration.

Figure 8- Performance of realistic filters and the FT, to be used in a CO detector. a) Realistic filter performance due to Hawkins 2003; b) FT spectra of the filters in the region of $2nd = 0.28$.

Figure 9- Simulated performance of an ideal filter and two filters with manufacturing errors.

Figure 10- Detail of the Fourier Transform magnitude of the ideal filter and the others with layers thicknesses errors, at the region of the fundamental Airy function ($2nd$=0.56 cm).

Figure 11- Average Amplitude Modulation as function of the CO_2 concentration considering the ideal filter and the others with manufacturing errors.

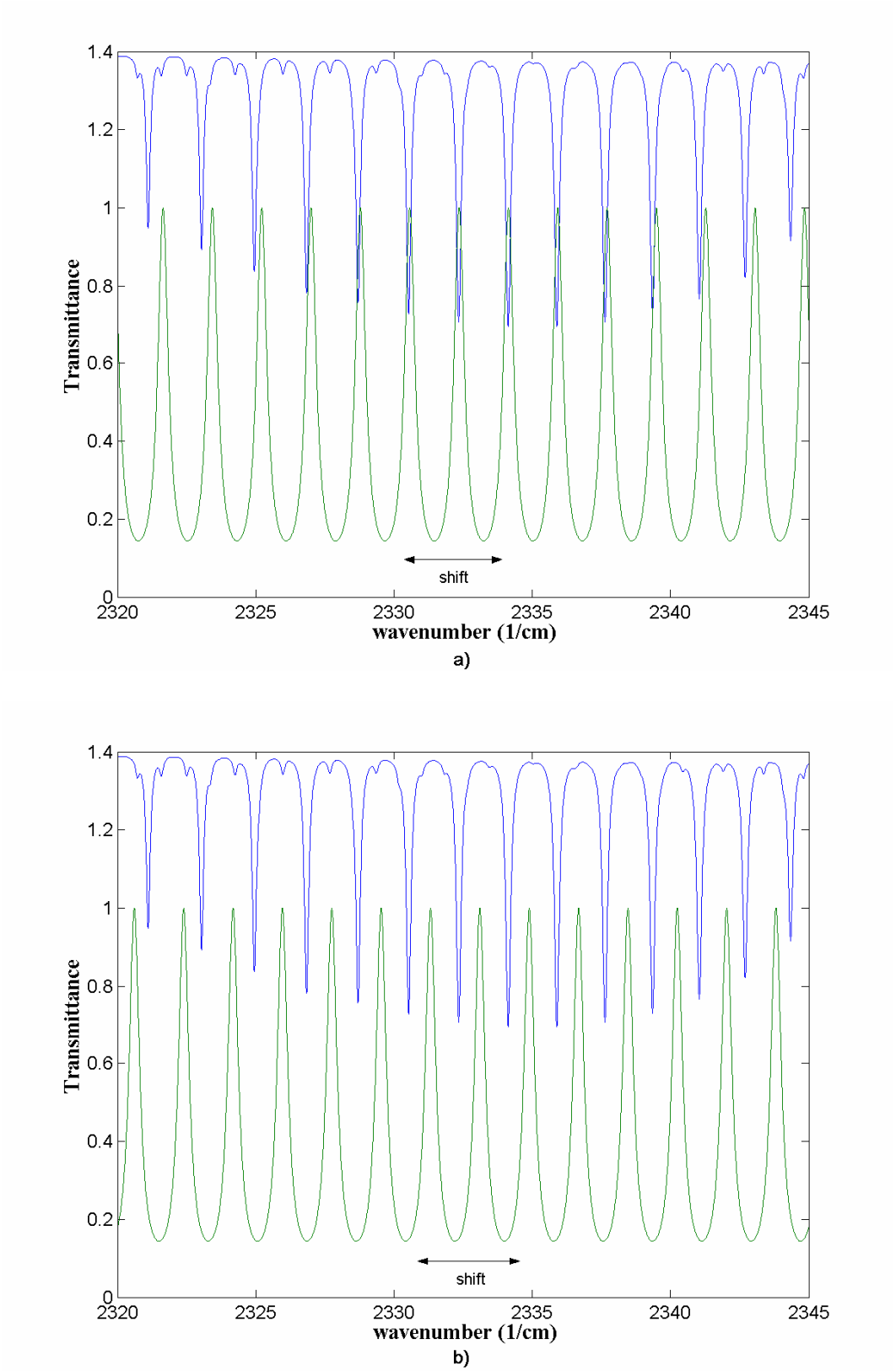

Figure 1- FPI's fringes and rotational lines due to CO_2. a) Absorption lines are matched to the FPI's fringes. b) FPI's fringes shifted along the wavenumber axis. The CO_2 spectrum is shifted up 0.4 units for clarity.

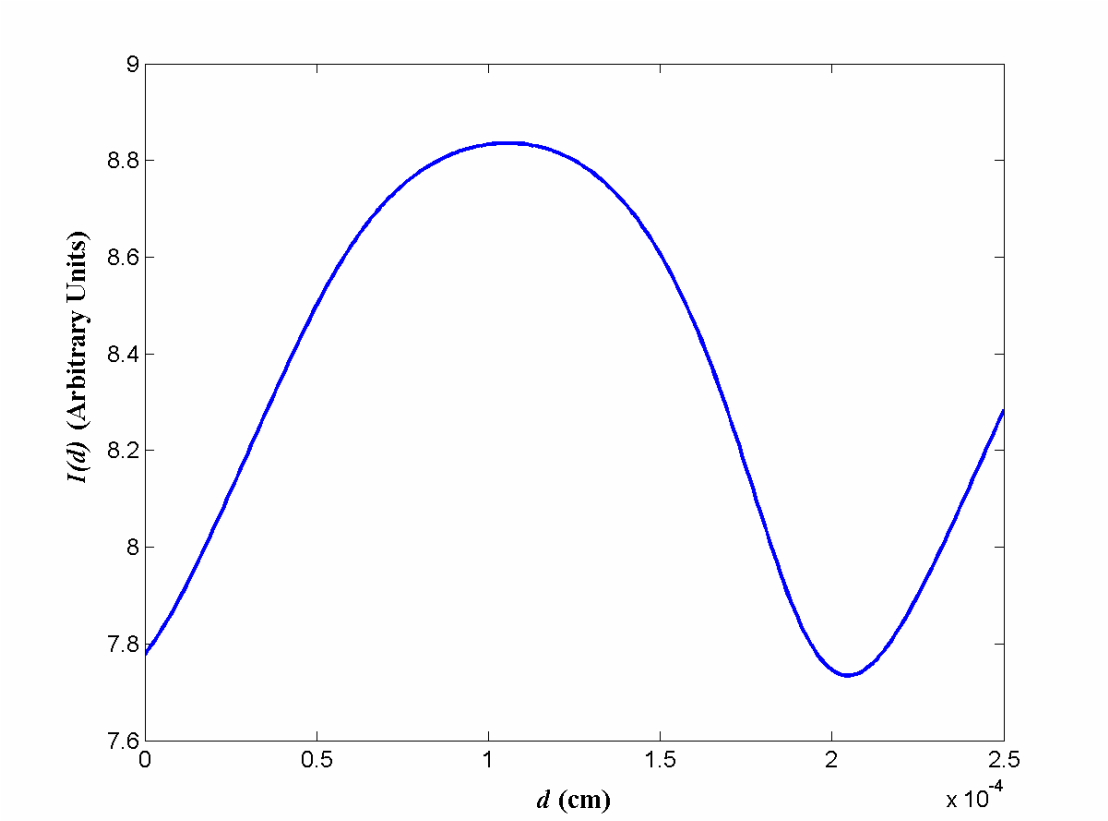

Figure 2- Simulated transmission through the system as a function of the cavity length *d*.

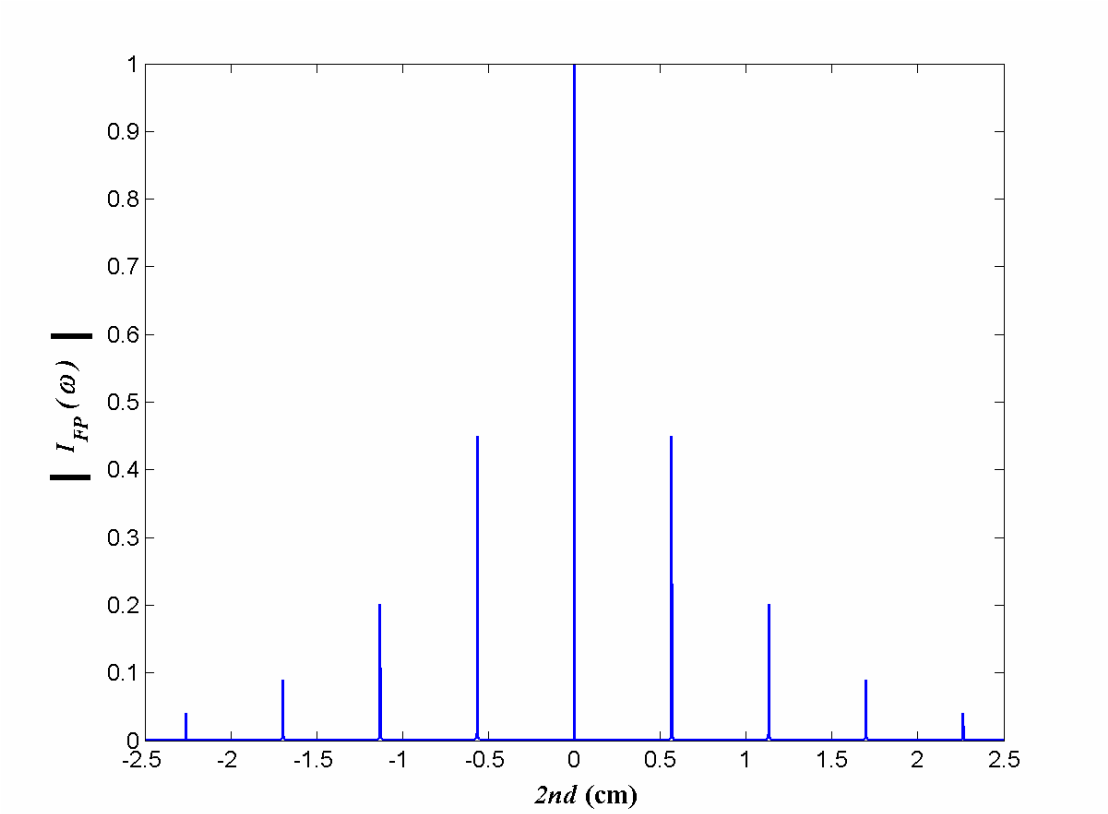

Figure 3- Fourier Transform of the Airy Function.

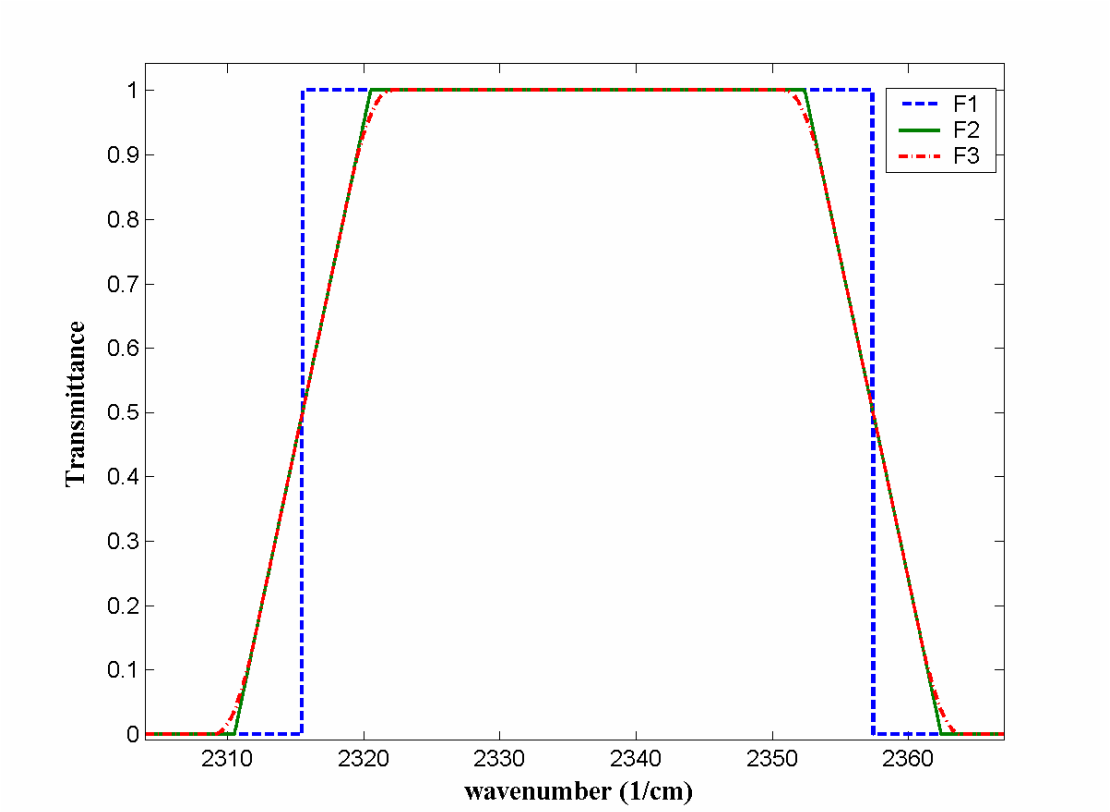

Figure 4- Simulated performance of three ideal filters.

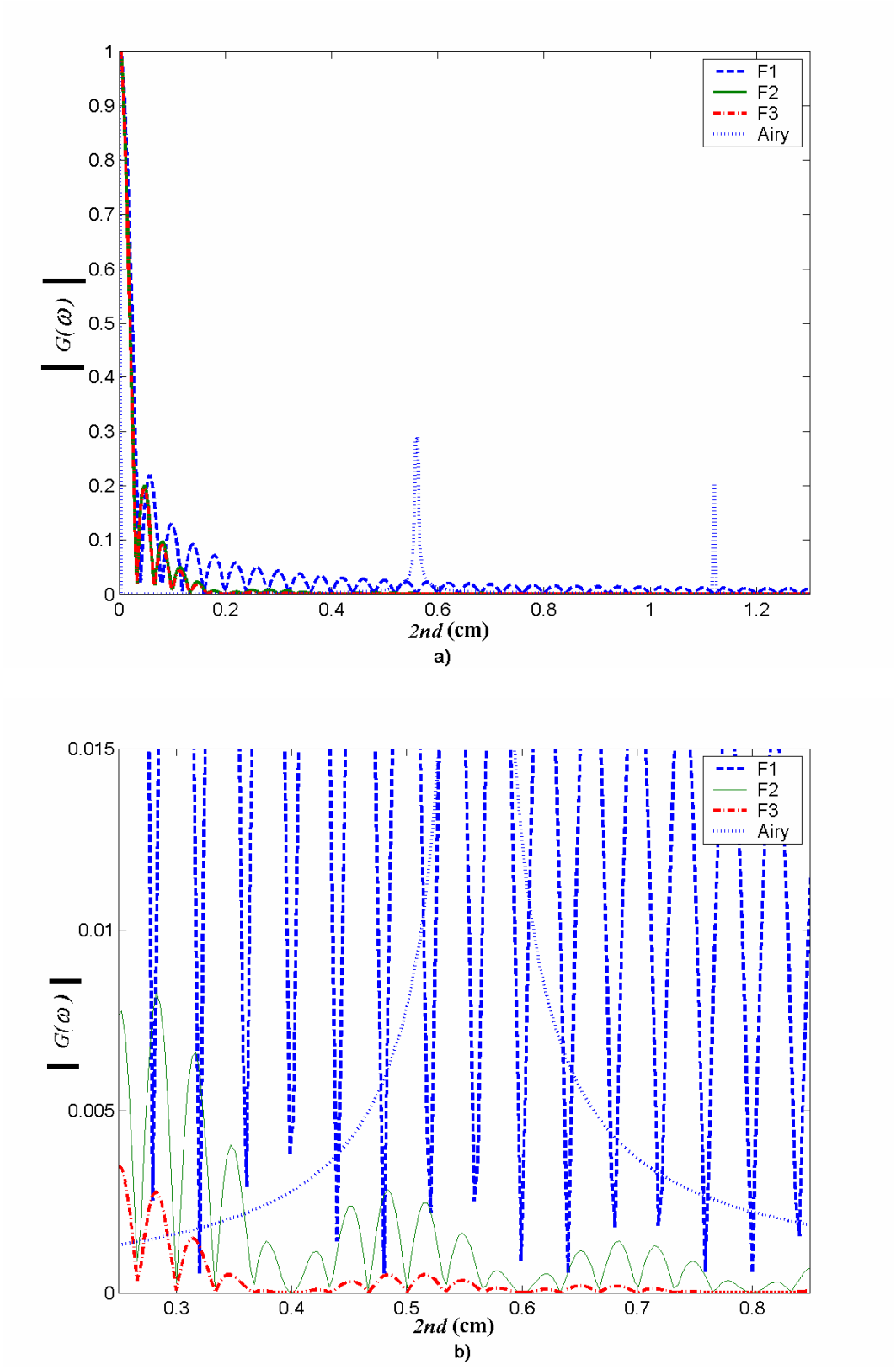

Figure 5- Fourier Transforms of both the ideal filters and the Airy Function. a) Positive frequencies of all the spectra; b) detail of the filter spectrum in the region of the fundamental frequency of the Airy Function.

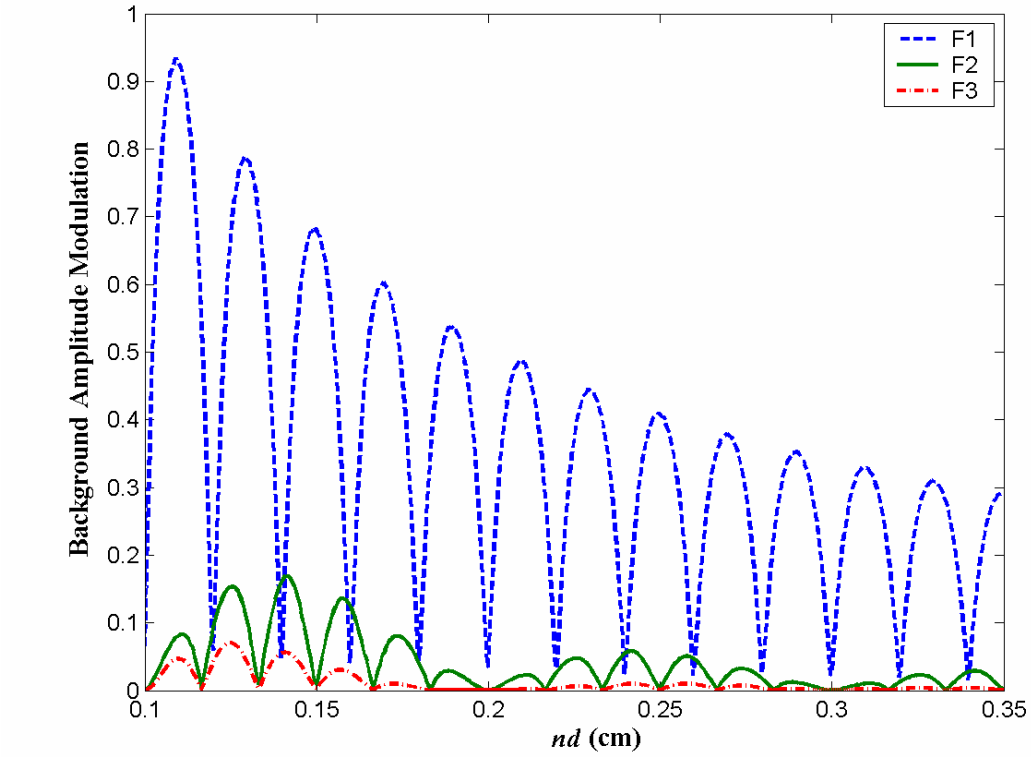

Figure 6- Background Amplitude Modulation as a function of *nd*.

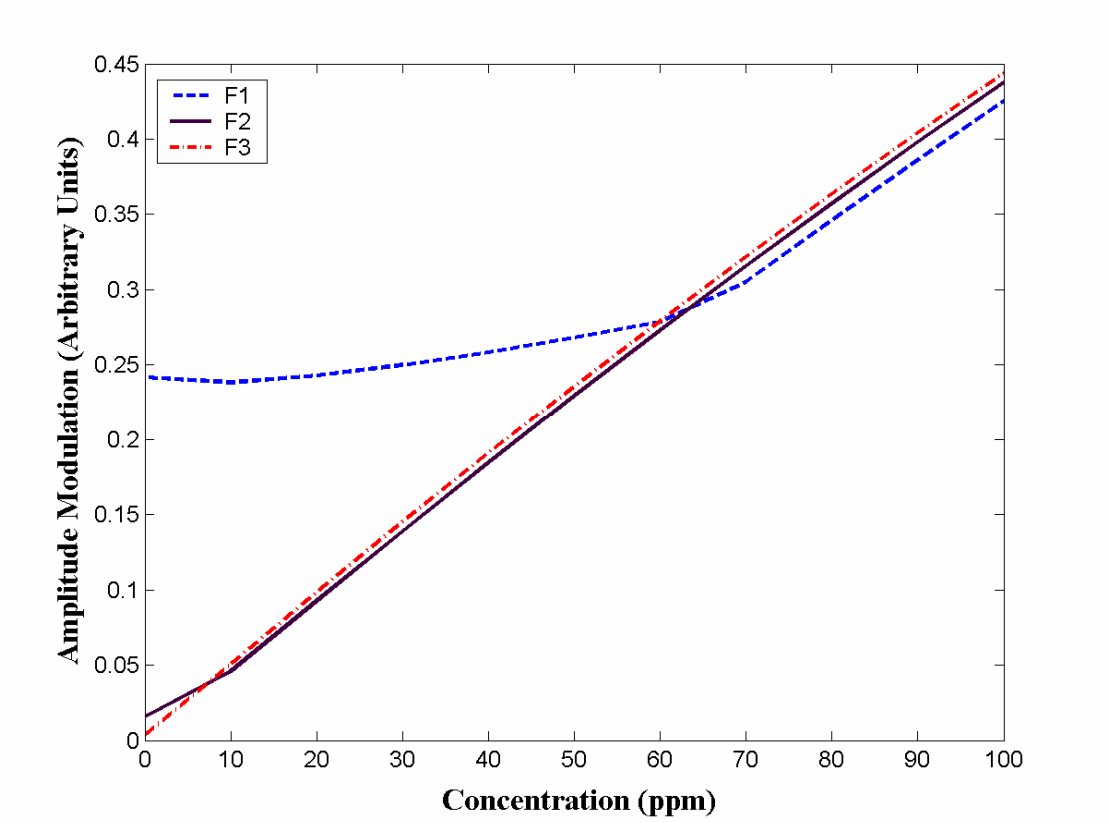

Figure 7- Amplitude Modulation as a function of the gas concentration.

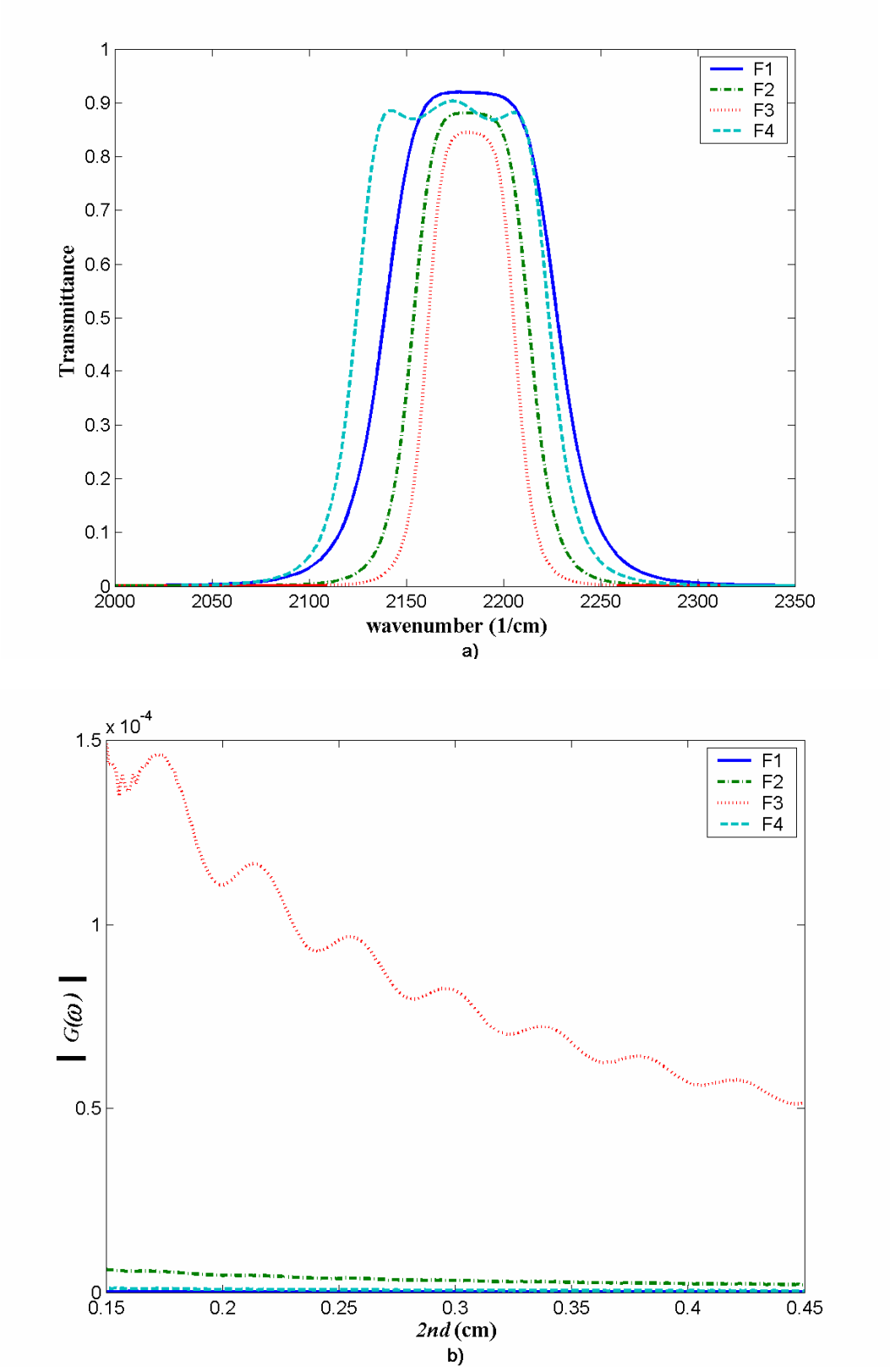

Figure 8- Performance of realistic filters and the FT, to be used in a CO detector. a) Realistic filter performance due to Hawkins 2003; b) FT spectra of the filters in the region of $2nd = 0.28$.

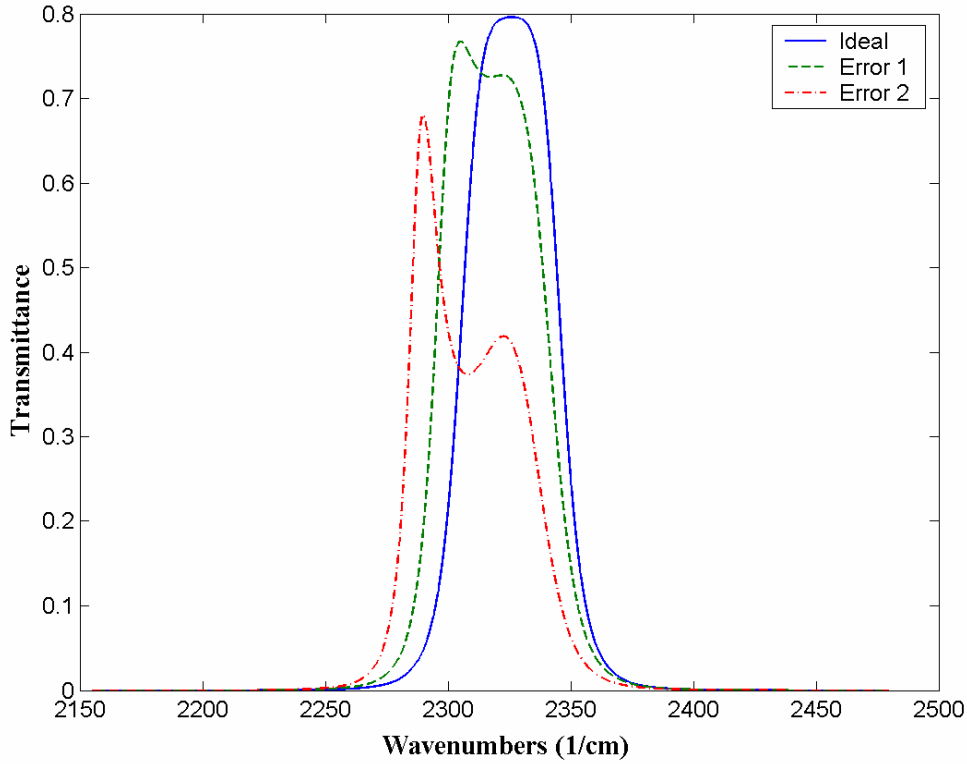

Figure 9- Simulated performance of an ideal filter and two others filters with manufacturing errors.

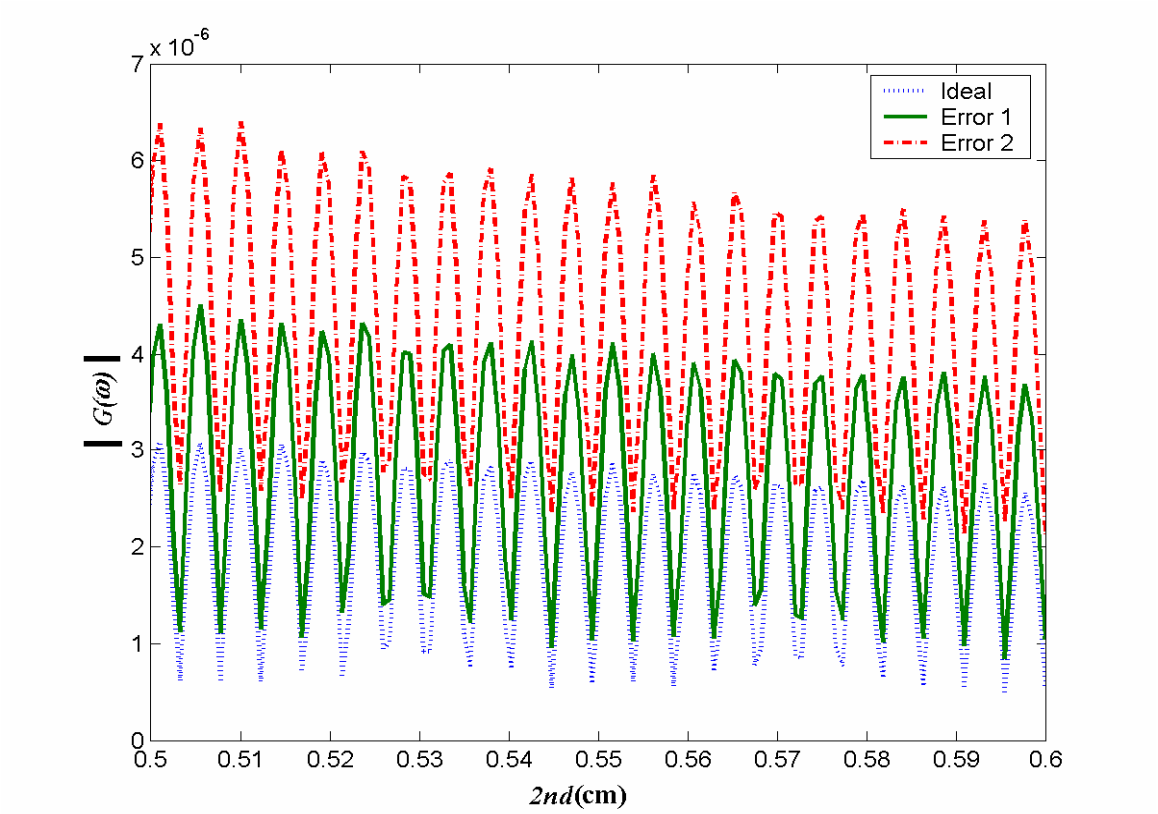

Figure 10- Detail of the Fourier Transform magnitude of the ideal filter and the others with layers thicknesses errors, at the region of the fundamental Airy function (2*nd*=0.56 cm).

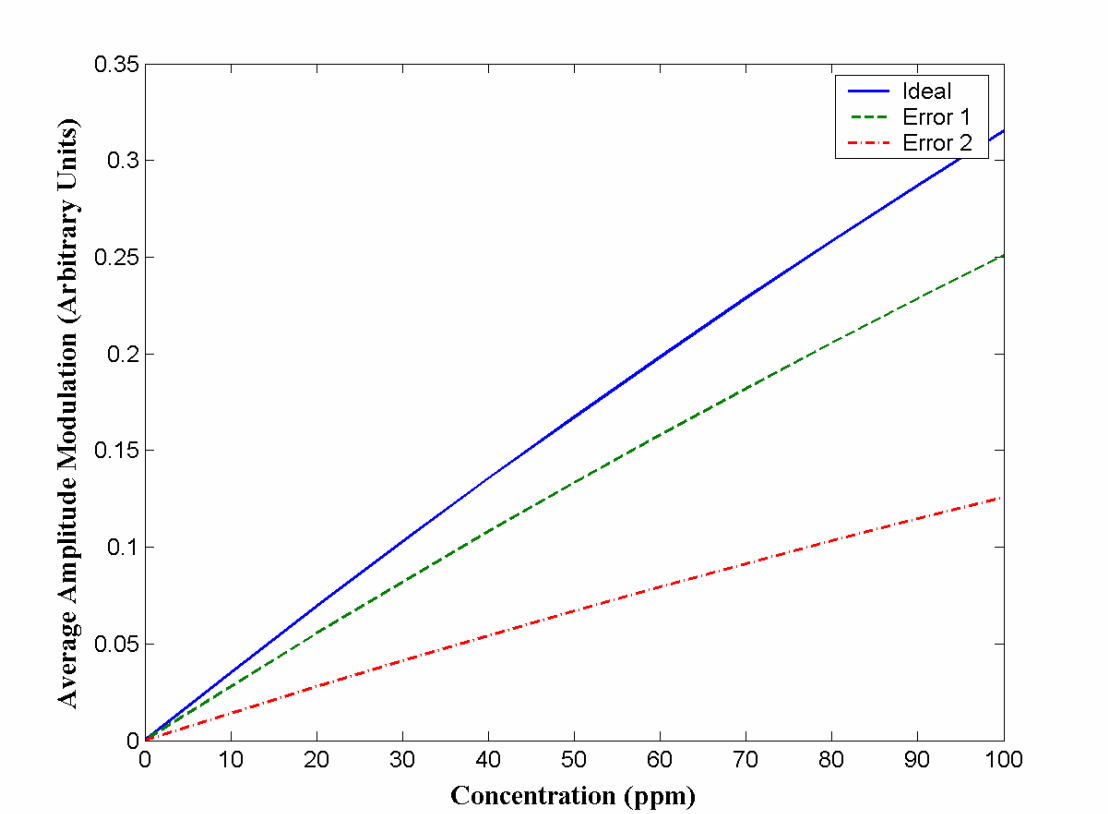

Figure 11- Average Amplitude Modulation as function of the CO_2 concentration considering the ideal filter and the others with manufacturing errors.